Silicon (2024) 16:3205–3216
https://doi.org/10.1007/s12633-024-02892-2

RESEARCH

Comparative Study of Entropies in Silicate and Oxide Frameworks

Micheal Arockiaraj[1] · J. Celin Fiona[1] · Arul Jeya Shalini[2]

Received: 13 December 2023 / Accepted: 1 February 2024 / Published online: 22 February 2024
© The Author(s), under exclusive licence to Springer Nature B.V. 2024

Abstract

Silicate and oxide frameworks are pervasive materials with remarkable structural complexity and tunability, offering a wide range of applications in catalysis, gas storage, drug delivery, electronics, and environmental remediation. Topological indices, which are mathematical representations of molecular structure, and Shannon entropy, a measure of information content, have emerged as powerful tools for studying the structural characteristics of these frameworks. In this study, we investigate the effectiveness of topological indices and entropy levels in revealing the structural characteristics of silicate and oxide frameworks. We formulate topological expressions for newly developed hybrid indices derived from geometric, harmonic, and Zagreb indices and conduct a scaled bond-wise comparative analysis between the two frameworks.

Keywords Silicate and oxide frameworks · Degree and degree-sum indices · Information function · Entropies

1 Introduction

Silica minerals, the most prevalent minerals in Earth's crust, hold immense geological significance, exhibiting unique versatility as they emerge from diverse environments, ranging from high-temperature igneous settings to low aquatic conditions [1]. Among these minerals, quartz stands out as one of the most widely utilized and recognized [2]. Silica minerals, primarily composed of silicon dioxide (SiO_2), serve as a subset of the larger class of silicate minerals. They form a broader and more widespread category, incorporating silicon, oxygen, and additional metallic elements such as aluminum, iron, magnesium, potassium, sodium, and calcium [3, 4]. Their prevalence and complexity are essential for understanding plate tectonics, mineral formation, and the earth's geological history. The basic structural unit of silicate minerals is the silicon-oxygen tetrahedron (SiO_4), which provides the basis for the vast diversity of silicate structures, ranging from isolated tetrahedra to intricate three-dimensional frameworks [5–7]. Silicate materials, especially zeolites, are used in environmental applications such as water purification and air pollution control. They contribute to reducing environmental pollutants and enhancing water quality [8]. Oxide frameworks constitute a diverse class of materials primarily composed of oxygen (O). Metal oxides like titanium dioxide and cerium oxide exhibit heterogeneous catalysis, influencing reactions in environmental cleanup and industrial processes [9–13].

In recent years, researchers have been exploring 2-dimensional, silicate, and oxide frameworks in various areas to broaden the scope of their applications [14–33] where Fig. 1 shows the 2-D view of the SiO_4 tetrahedron. Depending on the arrangement of tetrahedra, various silicate structures can be identified, including chain silicates, sheet silicates, framework silicates, and cyclic silicates [5]. The unit block of silicates is formed by placing six units of SiO_4 in a cyclic order as shown in Fig. 2a, and the removal of oxygen atoms in silicates gives the oxide unit as shown in Fig. 2b.

Topological indices serve as essential tools in mathematical chemistry, providing quantitative measures of molecular structure and offering a graph-theoretical approach to characterize the structural complexities of molecules. They represent a mathematical concept derived from molecular graphs, gaining prominence in QSAR/QSPR studies. These indices encode structural information and connectivity patterns within molecules, facilitating predictions of biological activities and physicochemical properties [34–40]. In QSAR and QSPR studies, topological indices serve as valuable tools for assimilating and predicting complex molecular behaviors,

✉ Micheal Arockiaraj
marockiaraj@gmail.com

1 Department of Mathematics, Loyola College, Chennai 600034, India

2 Department of Mathematics, Women's Christian College, Chennai 600006, India

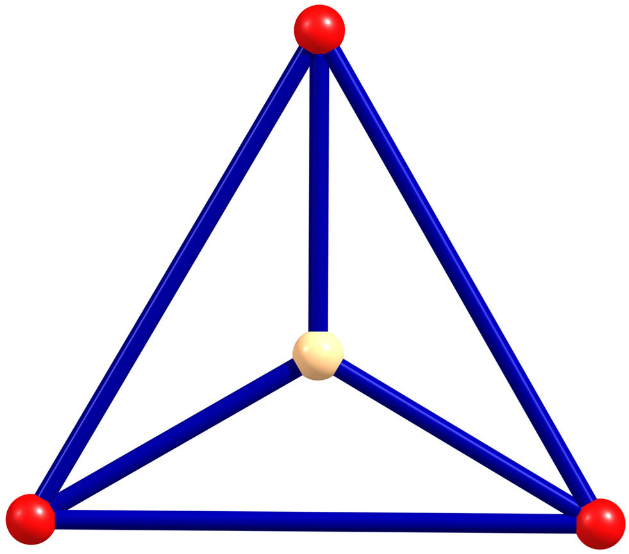

Fig. 1 2-dimensional view of SiO_4 tetrahedron

with applications in drug design, environmental chemistry, and materials engineering [40–45]. Topological indices are classified into three main types, including degree, distance, and eigenvalues of graphs. Exploring topological indices for silicate and oxide frameworks is essential for interpreting the structural features of these materials and their wide-ranging properties. Numerous research articles have already examined both distance-based [16, 17] and degree-based indices [18–31]. However, to our knowledge, no work has been reported on entropy indices.

Shannon entropy is a promising tool for describing the information content of molecules in the field of molecular analysis [46–48]. This approach offers the advantages of deriving a numerical value, facilitating easier comparisons among different molecules, and obviating the need for cumbersome, high-dimensional, and computationally intensive matrix processing. Their ability to quantify information content has drawn significant interest across various fields in recent years [49–54]. This paper explores the formulation of topological expressions for recently proposed hybrid indices based on geometric, harmonic, and Zagreb degree-based indices, emphasizing their efficacy in determining bond-wise entropy measures along with comparison between silicate and oxide frameworks.

2 Computational Techniques

We provide the graph theoretical parameters to describe the topological indices and entropies. Our study primarily focuses on topological indices, including geometric, harmonic, and Zagreb, along with their hybrid counterparts. These indices serve to quantify the entropies of silicate and oxide frameworks. We represent these chemical frameworks as connected graphs, where vertices symbolize atoms and edges represent chemical bonds between two atoms. The atoms and bonds of frameworks are generally grouped into sets $V(G)$ and $E(G)$, respectively, for a chemical graph G.

The vertex degree of $a \in V(G)$, denoted as $d_G(a)$, represents the count of neighboring vertex members associated with vertex a. Additionally, we define the degree-sum of the vertex a as $s_G(a)$, which is determined by adding the degrees of vertex members within the neighborhood of a. That is, $s_G(a) = \sum_{p \in N_G(a)} d_G(p)$ in which we used $N_G(a) = \{p \in V(G) \mid pa \in E(G)\}$. Let $d_{(p,a)}(G) = |\{ij \in E(G) : d_G(i) = p \text{ and } d_G(j) = a\}|$ and $s_{(p,a)}(G) = |\{ij \in E(G) : s_G(i) = p \text{ and } s_G(j) = a\}|$.

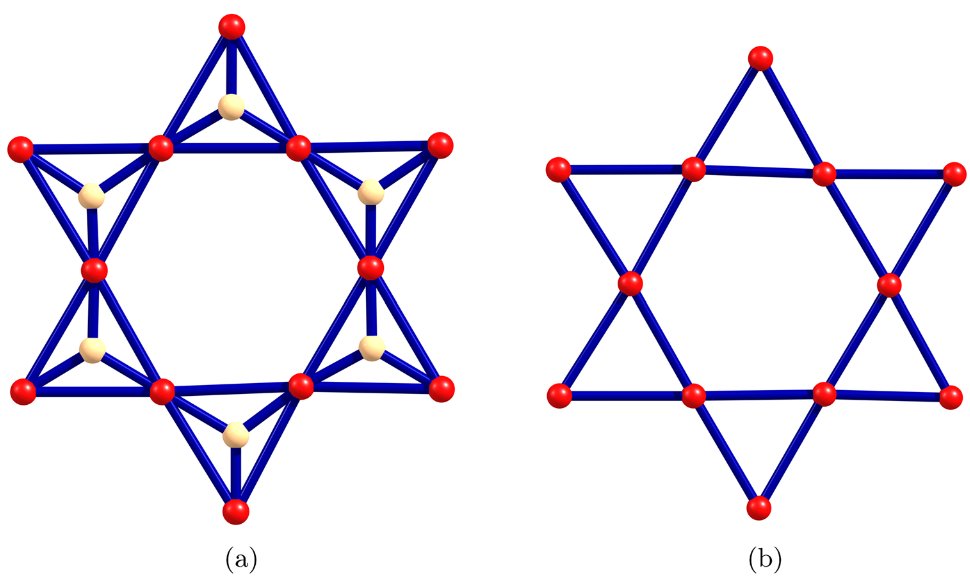

Fig. 2 Unit blocks (a) silicate (b) oxide

Consequently, the total number of edges in G would be structured into distinct partition classes in accordance with symmetrical criteria of $d_{(p,a)}(G)$ and $s_{(p,a)}(G)$, with these partition classes referred to as $D(G)$ and $S(G)$, respectively.

The degree and degree-sum metrics of G can be readily converted into numerical indices through the utilization of a designated index function denoted as χ. This function is formulated by employing two distinct mathematical operations, as outlined below [30, 31, 35, 55–58].

$$\chi^{d}(G) = \sum_{d_{(p,a)}(G)\in D(G)} d_{(p,a)}(G)\chi(p,a)$$

$$\chi^{d*}(G) = \prod_{d_{(p,a)}(G)\in D(G)} d_{(p,a)}(G)\chi(p,a)$$

$$\chi^{s}(G) = \sum_{s_{(p,a)}(G)\in S(G)} s_{(p,a)}(G)\chi(p,a)$$

$$\chi^{s*}(G) = \prod_{s_{(p,a)}(G)\in S(G)} s_{(p,a)}(G)\chi(p,a)$$

The bond additive and scalar multiplicative indices defined above, which correspond to self-powered index functions, are presented as follows.

$$\chi^{dp}(G) = \sum_{d_{(p,a)}(G)\in D(G)} d_{(p,a)}(G)\chi(p,a)^{\chi(p,a)}$$

$$\chi^{dp*}(G) = \prod_{d_{(p,a)}(G)\in D(G)} d_{(p,a)}(G)\chi(p,a)^{\chi(p,a)}$$

$$\chi^{sp}(G) = \sum_{s_{(p,a)}(G)\in S(G)} s_{(p,a)}(G)\chi(p,a)^{\chi(p,a)}$$

$$\chi^{sp*}(G) = \prod_{s_{(p,a)}(G)\in S(G)} s_{(p,a)}(G)\chi(p,a)^{\chi(p,a)}$$

The index function $\chi(p,a)$ for geometric, harmonic, and Zagreb, along with their respective hybrid indices is given below [38].

- Geometric $G(p,a) = \sqrt{pa}$
- Harmonic $H(p,a) = \dfrac{2}{p+a}$
- Bi-Zagreb $BM(p,a) = p + a + pa$
- Tri-Zagreb $TM(p,a) = p^2 + a^2 + pa$
- Geometric − Harmonic $GH(p,a) = \frac{\sqrt{pa}(p+a)}{2}$
- Geometric − Bi-Zagreb $GBM(p,a) = \frac{\sqrt{pa}}{p+a+pa}$
- Harmonic − Bi-Zagreb $HBM(p,a) = \frac{2}{(p+a+pa)(p+a)}$
- Harmonic − Tri-Zagreb $HTM(p,a) = \frac{2}{(p^2+a^2+pa)(p+a)}$
- Bi-Zagreb − Geometric $BMG(p,a) = \frac{(p+a+pa)}{\sqrt{pa}}$
- Bi-Zagreb − Harmonic $BMH(p,a) = \frac{(p+a+pa)(p+a)}{2}$
- Tri-Zagreb − Geometric $TMG(p,a) = \frac{p^2+a^2+pa}{\sqrt{pa}}$
- Tri-Zagreb − Harmonic $TMH(p,a) = \frac{(p^2+a^2+pa)(p+a)}{2}$

The above described index functions could be considered as the non-negative real valued structural information function χ on $E(G)$ in order to calculate the entropies of a graph G with degree and degree-sum metrics. Let $E(G) = \{c_1, c_2, ..., c_r\}$. The graph entropy of G is determined as follows:

$$\begin{aligned} I_\chi(G) &= -\sum_{i=1}^{r} \frac{\chi(c_i)}{\sum_{j=1}^{r}\chi(c_j)} \log\left(\frac{\chi(c_i)}{\sum_{j=1}^{r}\chi(c_j)}\right) \\ &= \log\left(\sum_{i=1}^{r}\chi(c_i)\right) - \frac{1}{\sum_{i=1}^{r}\chi(c_i)} \log\left(\prod_{i=1}^{r}\chi(c_i)^{\chi(c_i)}\right) \end{aligned}$$

As discussed in series of papers in recent years [51–53, 59–61], the substitution of the multiplicative component with a scalar multiplicative index has been considered. Therefore,

$$I_\chi(G) = \log(\chi(G)) - \frac{1}{\chi(G)} \log(\chi^{p*}(G))$$

The significance of entropy generally depends on the specific system being considered. In a thermodynamic context, smaller entropy suggests a more ordered and structured state, while in information theory, it implies that information is more predictable or less uncertain.

3 Results and Discussion

The foundation of silicate frameworks comprises (SiO_4) tetrahedra, which combine in diverse ways to create various peripheral configurations, including chain, cyclic, hexagonal, rhombic, and trapezium shaped networks of silicates. In our study, we analyze the prevalent hexagonal framework, resembling honeycomb benzene systems where each bond in this system is replaced by a tetrahedron.

We use the notation SL_n to represent silicate frameworks of dimension n. As mentioned earlier, the oxide frameworks (OX_n) are obtained as a byproduct of silicates, where each silicon and its associated bond are deleted. The three dimensional silicate and oxide frameworks are shown in Figs. 3 and 4.

The number of vertices and edges for silicate and oxide frameworks are ordered in the sets as $\{3(5n^2+n), 36n^2\}$ and $\{3(3n^2+n), 18n^2\}$, respectively. Silicate and oxide frameworks have been extensively covered in several papers [18–31] for computing various degree-based indices through bond partitions. We will utilize these partitions to derive the entropies for the first time and conduct a comparative analysis between them.

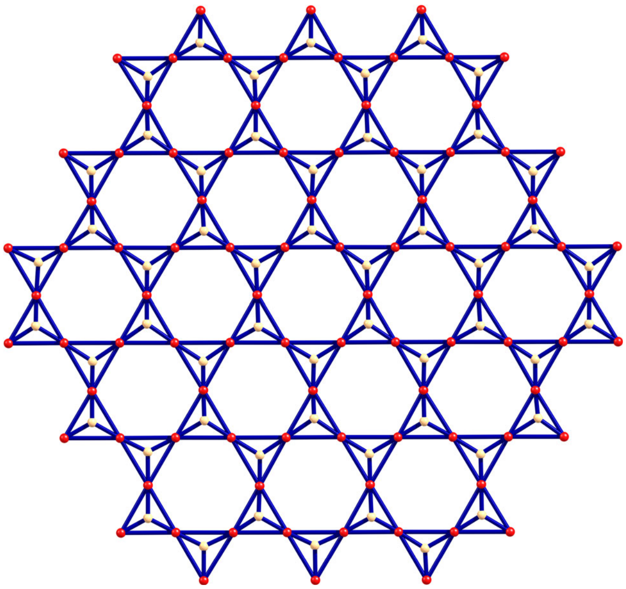

Fig. 3 Silicate framework SL_3

The bond partitions of silicate and oxide frameworks induced from degree parameters are given as $d_{(3,3)}(SL_n) = 6n, d_{(3,6)}(SL_n) = 18n^2+6n, d_{(6,6)}(SL_n) = 18n^2-12n$, and $d_{(2,4)}(OX_n) = 12n, d_{(4,4)}(OX_n) = 18n^2-12n$, respectively. Similarly, we tabulated the degree-sum bond distributions for silicate and oxide frameworks in Tables 1 and 2.

The degree and degree-sum index expressions for silicate and oxide frameworks can be represented by

$$\chi^{\{d,s\}}(G) = \begin{cases} \chi^d(G), \\ \chi^s(G) \end{cases}$$

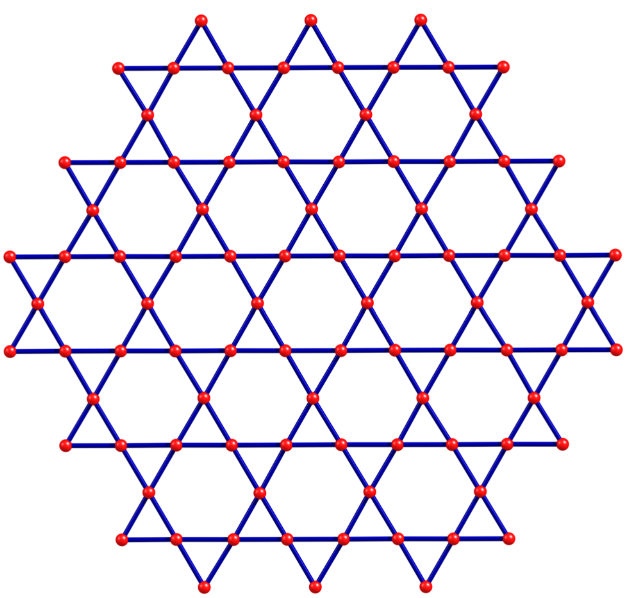

Fig. 4 Oxide framework OX_3

Table 1 Degree-sum partition of silicate frameworks

Bond X−Y	Degree-sum $s_{SL_n}(X) - s_{SL_n}(Y)$	Number of Bonds in SL_n
Si−O	15 − 15	$6n$
	15 − 24	24
	15 − 27	$24(n-1)$
	18 − 27	$12(n-1)$
	18 − 30	$18n^2 - 30n + 12$
O−O	24 − 27	12
	27 − 27	$3(4n-6)$
	27 − 30	$12(n-1)$
	30 − 30	$18n^2 - 36n + 18$

where $G \in \{SL_n, OX_n\}$. We now ready to compute the degree and degree-sum indices for the topological function χ, in which $\chi \in \{G, H, BM, TM, GH, GBM, HBM, HTM, BMG, BMH, TMG, TMH\}$. The indices are calculated using the following equations:

For degree type,

$$\begin{aligned}\chi^d(SL_n) &= d_{(3,3)}(SL_n)\,\chi(3,3) + d_{(3,6)}(SL_n)\,\chi(3,6) \\ &\quad + d_{(6,6)}(SL_n)\,\chi(6,6) \\ &= 6n\chi(3,3) + (18n^2+6n)\chi(3,6) \\ &\quad + (18n^2-12n)\chi(6,6),\end{aligned}$$

and for degree-sum type,

$$\begin{aligned}\chi^s(SL_n) &= s_{(15,15)}(SL_n)\,\chi(15,15) + s_{(15,24)}(SL_n)\,\chi(15,24) \\ &\quad + s_{(15,27)}(SL_n)\,\chi(15,27) + s_{(18,27)}(SL_n)\,\chi(18,27) \\ &\quad + s_{(18,30)}(SL_n)\,\chi(18,30) + s_{(24,27)}(SL_n)\,\chi(24,27) \\ &\quad + s_{(27,27)}(SL_n)\,\chi(27,27) + s_{(27,30)}(SL_n)\,\chi(27,30) \\ &\quad + s_{(30,30)}(SL_n)\,\chi(30,30) \\ &= 6n\chi(15,15) + 24\chi(15,24) + 24(n-1)\chi(15,27) \\ &\quad + 12(n-1)\chi(18,27) + (18n^2-30n+12)\chi(18,30) \\ &\quad + 12\chi(24,27) + 3(4n-6)\chi(27,27) + 12(n-1)\chi(27,30) \\ &\quad + (18n^2-36n+18)\chi(30,30).\end{aligned}$$

Table 2 Degree-sum partition of oxide frameworks

Bond X−Y	Degree-sum $s_{OX_n}(X) - s_{OX_n}(Y)$	Number of Bonds in OX_n
O−O	8 − 12	12
	8 − 14	$12(n-1)$
	12 − 14	12
	14 − 14	$3(4n-6)$
	14 − 16	$12(n-1)$
	16 − 16	$18n^2 - 36n + 18$

Result 1 Let SL_n be the silicate frameworks of dimension n where $n > 1$.

1. $$G^{\{d,s\}}(SL_n) = \begin{cases} (108+54\sqrt{2})n^2+(18\sqrt{2}-54)n, \\ (3(633318697598976(5+\sqrt{15})n^2 \\ +105553116266496(12\sqrt{5} \\ +6\sqrt{6}+6\sqrt{10}-10\sqrt{15}-37)n \\ +422212465065984\sqrt{15} \\ -633318697598976\sqrt{10} \\ -633318697598976\sqrt{6} \\ -1266637395197952\sqrt{5} \\ +1266637395197952\sqrt{2} \\ +2986965441045055)) \\ /17592186044416 \end{cases}$$

2. $$H^{\{d,s\}}(SL_n) = \begin{cases} (21n^2+4n)/3, \\ (7142499n^2+2601391n \\ +198126)/5290740 \end{cases}$$

3. $$BM^{\{d,s\}}(SL_n) = \begin{cases} 1350n^2-324n, \\ 27864n^2-13770n+702 \end{cases}$$

4. $$TM^{\{d,s\}}(SL_n) = \begin{cases} 3078n^2-756n, \\ 80352n^2-39474n+1350 \end{cases}$$

5. $$GH^{\{d,s\}}(SL_n) = \begin{cases} (243\sqrt{2}+648)n^2+(81\sqrt{2}-378)n, \\ (5769967165772584 5n^2 \\ -29037514943132454n \\ +1343876184123989)/ \\ 2199023255552 \end{cases}$$

6. $$GBM^{\{d,s\}}(SL_n) = \begin{cases} ((120\sqrt{2}+135)n^2+(40\sqrt{2}-18)n)/60, \\ 3((15656146628016 \\ \sqrt{15}+47946949048299)n^2 \\ +(10618009477824\sqrt{10} \\ -26093577713360\sqrt{15} \\ +17336749938368\sqrt{6} \\ +41189325356928\sqrt{5} \\ -30538219069302)n \\ +10437431085344\sqrt{15} \\ +20144945300032\sqrt{10} \\ -17336749938368\sqrt{6} \\ -41189325356928\sqrt{5} \\ +26339954841984\sqrt{2} \\ -4960029211893)/ \\ 255717061590928 \end{cases}$$

7. $$HBM^{\{d,s\}}(SL_n) = \begin{cases} 7(15n^2+2n)/5, \\ 9(36857178520121n^2 \\ +12720489145262n \\ +336745608377)/ \\ 63929265397732 \end{cases}$$

8. $$HTM^{\{d,s\}}(SL_n) = \begin{cases} 4(16n^2+3n)/7, \\ (4(3050143349481n^2 \\ +1095829472792n \\ +98072334141))/ \\ 6855826794705 \end{cases}$$

9. $$BMG^{\{d,s\}}(SL_n) = \begin{cases} (81\sqrt{2}+144)n^2+(27\sqrt{2}-66)n, \\ (6333186975989760 \\ \sqrt{3}(49+16\sqrt{15})n^2 \\ -35184372088832(\sqrt{5}(\sqrt{6} \\ (3\sqrt{10}(490+117\sqrt{15}) \\ -578\sqrt{15})-1770\sqrt{6}) \\ -17880)n+\sqrt{5}(\sqrt{6} \\ (\sqrt{10}(20688410788233216 \\ +15625577989437259\sqrt{15}) \\ -20336567067344896\sqrt{15}) \\ -62276338597232640 \\ \sqrt{6})-629096572948316160)/ \\ 527765581332480\sqrt{5} \end{cases}$$

10. $$BMH^{\{d,s\}}(SL_n) = \begin{cases} 7371n^2-2457n, \\ 772416n^2-518346n+42660 \end{cases}$$

11. $$TMG^{\{d,s\}}(SL_n) = \begin{cases} (189\sqrt{2}+324)n^2+(63\sqrt{2}-162)n, \\ (395824185999360 \\ \sqrt{2}(45+49\sqrt{3/5})n^2 \\ -13194139533312(-570\sqrt{3} \\ -604\sqrt{10}+490\sqrt{30} \\ +\sqrt{5}(345\sqrt{10}-542))n \\ +2586051348529152\sqrt{30}+\sqrt{5} \\ (5610180619004941\sqrt{10} \\ -7151223627055104) \\ -7969260278120448 \\ \sqrt{10}-7520659533987840\sqrt{3})/ \\ (10995116277760\sqrt{2}) \end{cases}$$

12. $$TMH^{\{d,s\}}(SL_n) = \begin{cases} 16767n^2-5589n, \\ 2220048n^2-1482138n \\ +109512 \end{cases}$$

We apply the bond partitions of oxide frameworks to derive the topological indices using the equations provided below. For degree type,

$$\begin{aligned}\chi^d(\mathrm{OX}_n) &= d_{(2,4)}(\mathrm{OX}_n)\ \chi(2,4) + d_{(4,4)}(\mathrm{OX}_n)\ \chi(4,4)\\ &= 12n\chi(2,4) + (18n^2 - 12n)\chi(4,4),\end{aligned}$$

and for degree-sum type,

$$\begin{aligned}\chi^s(\mathrm{OX}_n) = &\ s_{(8,12)}(\mathrm{OX}_n)\ \chi(8,12) + s_{(8,14)}(\mathrm{OX}_n)\ \chi(8,14)\\ &+ s_{(12,14)}(\mathrm{OX}_n)\ \chi(12,14)\ + s_{(14,14)}(\mathrm{OX}_n)\ \chi(14,14)\\ &+ s_{(14,16)}(\mathrm{OX}_n)\ \chi(14,16) + s_{(16,16)}(\mathrm{OX}_n)\ \chi(16,16)\\ = &\ 12\chi(8,12) + 12(n-1)\chi(8,14) + 12\chi(12,14)\\ &+ 3(4n-6)\chi(14,14)\ + 12(n-1)\chi(14,16)\\ &+ (18n^2 - 36n + 18)\chi(16,16).\end{aligned}$$

Result 2 Let OX_n be the oxide frameworks of dimension n where $n > 1$.

1. $G^{\{d,s\}}(\mathrm{OX}_n) = \begin{cases} 72n^2 + (24\sqrt{2} - 48)n, \\ 288n^2 + (48\sqrt{7} + 48\sqrt{14} - 408)n + 48\sqrt{6} \\ -48\sqrt{7} - 48\sqrt{14} + 24\sqrt{42} + 36 \end{cases}$
2. $H^{\{d,s\}}(\mathrm{OX}_n) = \begin{cases} (9n^2 + 2n)/2, \\ (45045n^2 + 19942n + 2861)/40040 \end{cases}$
3. $BM^{\{d,s\}}(\mathrm{OX}_n) = \begin{cases} 432n^2 - 120n, \\ 5184n^2 - 3024n + 216 \end{cases}$
4. $TM^{\{d,s\}}(\mathrm{OX}_n) = \begin{cases} 864n^2 - 240n, \\ 13824n^2 - 8016n + 408 \end{cases}$
5. $GH^{\{d,s\}}(\mathrm{OX}_n) = \begin{cases} 288n^2 + (72\sqrt{2} - 192)n, \\ (10133099161583616n^2 \\ +(1161084278931456\sqrt{7} \\ -9169941668475777)n \\ -1161084278931456\sqrt{7} \\ +3482709361307204)/ \\ 2199023255552 \end{cases}$
6. $GBM^{\{d,s\}}(\mathrm{OX}_n) = \begin{cases} (21n^2 + (12\sqrt{2} - 14)n)/7, \\ (191486536n^2 + 5626(12192 \\ \sqrt{7} + 6432\sqrt{14} - 42545)n \\ +23689056\sqrt{42} - 36186432 \\ \sqrt{14} - 68592192\sqrt{7} + 79235808 \\ \sqrt{6} - 23935817)/191486536 \end{cases}$
7. $HBM^{\{d,s\}}(\mathrm{OX}_n) = \begin{cases} (84n^2 + 16n)/7, \\ (191486536n^2 + 84969478n + \\ 3804919)/47871634 \end{cases}$
8. $HTM^{\{d,s\}}(\mathrm{OX}_n) = \begin{cases} (42n^2 + 8n)/7, \\ (265475847n^2 + 111022130n + \\ 19214171)/176983898 \end{cases}$
9. $BMG^{\{d,s\}}(\mathrm{OX}_n) = \begin{cases} 108n^2 + (42\sqrt{2} - 72)n, \\ (79798155897470976n^2 \\ +13405245765844992\sqrt{14}n \\ +14144117579710464\sqrt{7}n \\ -112308515707551744n- \\ 13405245765844992\sqrt{14} \\ -14144117579710464\sqrt{7} \\ +14284855068065792\sqrt{6} \\ +53102495442325371)/ \\ 246290604621824 \end{cases}$
10. $BMH^{\{d,s\}}(\mathrm{OX}_n) = \begin{cases} 1728n^2 - 648n, \\ 82944n^2 - 64848n + 7272 \end{cases}$
11. $TMG^{\{d,s\}}(\mathrm{OX}_n) = \begin{cases} 216n^2 + (84\sqrt{2} - 144)n, \\ 3(17732923532771328n^2 \\ +2973079441506304\sqrt{14}n \\ +3272146604261376\sqrt{7}n \\ -25121641671426048n \\ -2973079441506304\sqrt{14} \\ -3272146604261376\sqrt{7} \\ +19511122232716877)/ \\ 61572651155456 \end{cases}$
12. $TMH^{\{d,s\}}(\mathrm{OX}_n) = \begin{cases} 3456n^2 - 1296n, \\ 221184n^2 - 172800n + 17952 \end{cases}$

We now provide the multiplicative self-powered degree as well as degree-sum indices of silicate frameworks for determining the numerical values of entropies. We denote $SD = \{(3,3), (3,6), (6,6)\}$ and $SS = \{(15,15), (15,24), (15,27), (18,27), (18,30), (24,27), (27,27), (27,30), (30,30)\}$. Let $\alpha(\mathrm{SL}_n) = \prod_{(p,a)\in SD} \chi(p,a)^{\chi(p,a)}$ and $\beta(\mathrm{SL}_n) = \prod_{(p,a)\in SS} \chi(p,a)^{\chi(p,a)}$. Therefore, the mathematical expressions for silicate frameworks are given by

- $\chi^{dp*}(\mathrm{SL}_n) = \alpha(\mathrm{SL}_n)(1944n^5 - 648n^4 - 432n^3)$
- $\chi^{sp*}(\mathrm{SL}_n) = \beta(\mathrm{SL}_n)(23219011584n^9 - 189621927936n^8 + 673351335936n^7 - 1358312177664n^6 + 1702727516160n^5 - 1358312177664n^4 + 673351335936n^3 - 189621927936n^2 + 23219011584n)$

Similary, for oxide frameworks, we denote $OD = \{(2,4),(4,4)\}$, $OS = \{(8,12),(8,14),(12,14),(14,14),(14,16),(16,16)\}$, $\alpha(\mathrm{OX}_n) = \prod_{(p,a)\in OD} \chi(p,a)^{\chi(p,a)}$ and $\beta(\mathrm{OX}_n) = \prod_{(p,a)\in OS} \chi(p,a)^{\chi(p,a)}$. Therefore, the mathematical expressions for oxide frameworks are given by

- $\chi^{dp*}(\mathrm{OX}_n) = \alpha(\mathrm{OX}_n)(216n^3 - 144n^2)$
- $\chi^{sp*}(\mathrm{OX}_n) = \beta(\mathrm{OX}_n)(4478976n^5 - 24634368n^4 + 53747712n^3 - 58226688n^2 + 31352832n - 6718464)$

As we can observe, the entropy formula involves incorporating mathematical expressions of topological indices and self-powered topological indices. The resulting mathematical expressions are longer in terms of dimension n. Therefore, we calculate the numerical entropy values for degree and degree-sum index expressions for silicate and oxide frameworks at some fixed dimensions n, which are provided in Tables 3 and 4.

Data scaling is an essential preprocessing step in various machine learning and statistical algorithms. Its primary objective is to transform the features of a dataset into a comparable scale, thereby preventing any single feature from unduly influencing the learning process of the models. The necessity for data scaling emerges from the distinct units, magnitudes, and ranges characterizing features within a dataset, potentially impeding the performance of models. As seen from our entropy calculations, the entropies of silicate and oxide frameworks have been computed based on the total number of bonds within those frameworks, which are not of equal quantity. Hence, we calculate the bond-wise entropy by scaling the total entropy through division by the number

Table 3 Entropies based on $\chi^d(\mathrm{SL}_n)$ and $\chi^s(\mathrm{SL}_n)$ of silicate frameworks

χ	d s	$n=4$	$n=5$	$n=6$	$n=7$	$n=8$	$n=9$	$n=10$	$n=11$	$n=12$
G		7.938	8.396	8.769	9.082	9.353	9.591	9.804	9.997	10.172
		9.515	9.994	10.379	10.700	10.976	11.218	11.434	11.628	11.806
H		4.651	5.122	5.501	5.819	6.091	6.331	6.545	6.737	6.913
		1.775	2.617	3.221	3.685	4.058	4.370	4.638	4.871	5.079
BM		9.902	10.367	10.743	11.060	11.332	11.572	11.786	11.980	12.156
		12.786	13.294	13.695	14.026	14.309	14.557	14.776	14.974	15.154
TM		10.722	11.189	11.566	11.882	12.155	12.395	12.609	12.803	12.979
		13.832	14.345	14.748	15.081	15.365	15.613	15.834	16.032	16.212
GH		9.588	10.054	10.431	10.748	11.021	11.261	11.475	11.669	11.845
		12.725	13.233	13.633	13.993	14.269	14.496	14.715	14.913	15.093
GBM		4.267	4.756	5.146	5.470	5.748	5.991	6.207	6.402	6.580
		1.614	2.488	3.110	3.586	3.968	4.286	4.557	4.794	5.005
HBM		5.811	6.262	6.630	6.940	7.207	7.443	7.654	7.845	8.019
		4.155	4.688	5.105	5.446	5.736	5.987	6.209	6.408	6.589
HTM		4.944	5.408	5.782	6.096	6.367	6.605	6.817	7.009	7.184
		2.392	3.132	3.674	4.097	4.444	4.736	4.988	5.210	5.409
BMG		8.288	8.744	9.115	9.427	9.697	9.935	10.147	10.339	10.514
		9.593	10.071	10.455	10.776	11.052	11.294	11.509	11.704	11.880
BMH		11.569	12.041	12.422	12.741	13.016	13.258	13.473	13.668	13.845
		16.018	16.553	16.969	17.310	17.599	17.851	18.075	18.275	18.457
TMG		9.111	9.567	9.939	10.252	10.522	10.760	10.973	11.165	11.340
		10.635	11.121	11.508	11.831	12.108	12.351	12.568	12.763	12.940
TMH		12.388	12.861	13.243	13.562	13.837	14.079	14.295	14.489	14.666
		17.062	17.602	18.02	18.362	18.653	18.905	19.129	19.330	19.512

Table 4 Entropies based on $\chi^d(OX_n)$ and $\chi^s(OX_n)$ of oxide frameworks

χ	d / s	$n=4$	$n=5$	$n=6$	$n=7$	$n=8$	$n=9$	$n=10$	$n=11$	$n=12$
G		6.983	7.445	7.820	8.135	8.406	8.646	8.859	9.052	9.228
		8.291	8.776	9.163	9.487	9.764	10.007	10.224	10.420	10.597
H		4.217	4.687	5.065	5.381	5.654	5.893	6.106	6.299	6.474
		2.030	2.742	3.268	3.680	4.019	4.305	4.554	4.773	4.969
BM		8.750	9.218	9.596	9.914	10.187	10.428	10.642	10.836	11.013
		11.080	11.593	11.997	12.331	12.616	12.865	13.086	13.284	13.464
TM		9.440	9.909	10.288	10.606	10.880	11.120	11.335	11.529	11.706
		12.045	12.564	12.972	13.307	13.593	13.843	14.064	14.263	14.444
GH		8.337	8.806	9.185	9.504	9.778	10.019	10.234	10.428	10.605
		11.048	11.473	11.877	12.211	12.497	12.745	12.966	13.165	13.345
GBM		3.730	4.223	4.615	4.941	5.219	5.463	5.680	5.875	6.052
		1.765	2.521	3.074	3.504	3.854	4.149	4.404	4.628	4.828
HBM		5.260	5.710	6.077	6.386	6.653	6.889	7.099	7.290	7.463
		4.005	4.507	4.905	5.234	5.515	5.759	5.977	6.173	6.351
HTM		4.525	4.988	5.362	5.676	5.947	6.185	6.397	6.589	6.764
		2.559	3.199	3.681	4.065	4.383	4.656	4.893	5.105	5.294
BMG		7.408	7.867	8.238	8.551	8.822	9.060	9.273	9.465	9.640
		8.417	8.901	9.287	9.610	9.887	10.130	10.346	10.541	10.718
BMH		10.105	10.581	10.963	11.284	11.560	11.802	12.018	12.213	12.390
		13.763	14.302	14.721	15.064	15.355	15.609	15.833	16.034	16.217
TMG		8.010	8.559	8.931	9.244	9.515	9.753	9.966	10.158	10.333
		9.384	9.873	10.262	10.587	10.865	11.108	11.325	11.520	11.698
TMH		10.794	11.271	11.655	11.976	12.252	12.495	12.711	12.906	13.083
		14.729	15.274	15.696	16.041	16.333	16.587	16.812	17.014	17.196

Table 5 Scaled entropy values of silicate and oxide frameworks based on degree indices

χ^d	SL_4	OX_4	SL_5	OX_5	SL_6	OX_6	SL_7	OX_7
G	0.01378	0.02425	0.00933	0.01654	0.00677	0.01207	0.00515	0.00922
H	0.00807	0.01464	0.00569	0.01042	0.00425	0.00782	0.00330	0.00610
BM	0.01719	0.03038	0.01152	0.02049	0.00829	0.01481	0.00627	0.01124
TM	0.01862	0.03278	0.01243	0.02202	0.00892	0.01588	0.00674	0.01203
GH	0.01665	0.02895	0.01117	0.01957	0.00805	0.01418	0.00609	0.01078
GBM	0.00741	0.01295	0.00529	0.00938	0.00397	0.00712	0.00310	0.00560
HBM	0.01009	0.01826	0.00696	0.01269	0.00512	0.00938	0.00393	0.00724
HTM	0.00858	0.01571	0.00601	0.01109	0.00446	0.00828	0.00346	0.00644
BMG	0.01439	0.02572	0.00972	0.01748	0.00703	0.01271	0.00534	0.00970
BMH	0.02009	0.03509	0.01338	0.02351	0.00959	0.01692	0.00722	0.01279
TMG	0.01582	0.02812	0.01063	0.01902	0.00767	0.01378	0.00581	0.01048
TMH	0.02151	0.03748	0.01429	0.02505	0.01022	0.01799	0.00769	0.01358

Fig. 5 Comparative graphs of scaled degree entropies between SL_n and OX_n

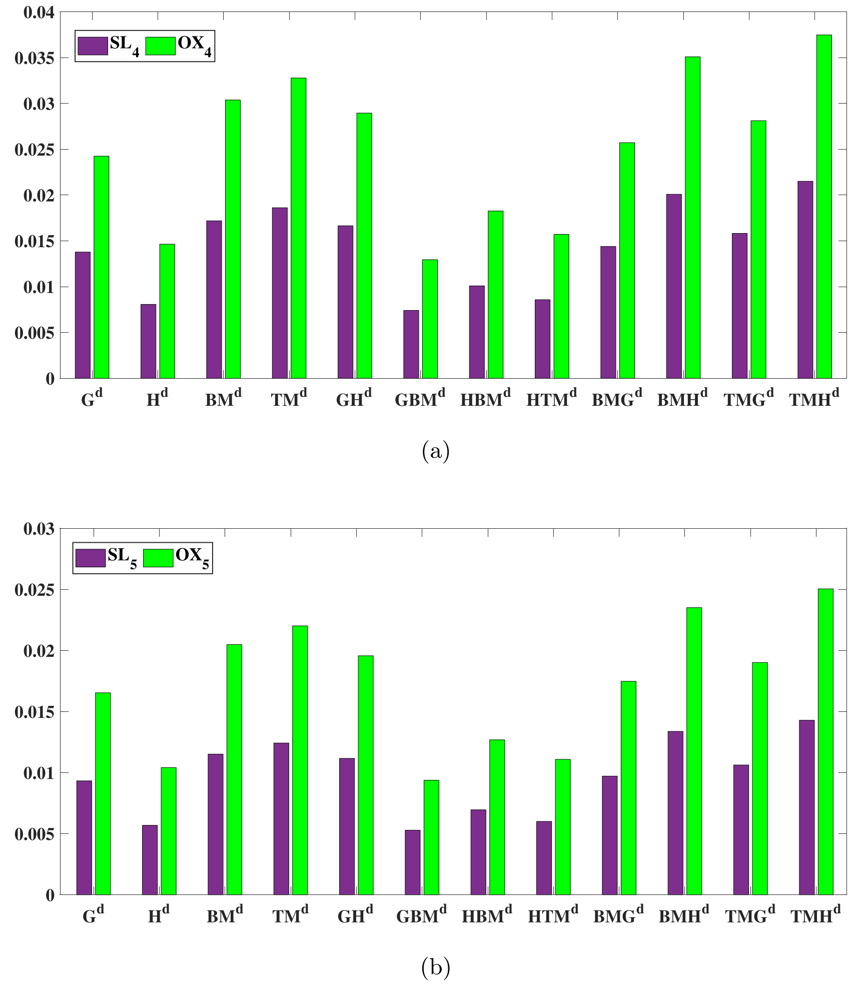

Table 6 Scaled entropy values of silicate and oxide frameworks based on degree-sum indices

χ^s	SL_4	OX_4	SL_5	OX_5	SL65	OX_6	SL_7	OX_7
G	0.01652	0.02879	0.01111	0.01950	0.00801	0.01414	0.00607	0.01076
H	0.00308	0.00705	0.00291	0.00609	0.00249	0.00504	0.00209	0.00417
BM	0.02220	0.03847	0.01477	0.02576	0.01057	0.01851	0.00795	0.01398
TM	0.02401	0.04182	0.01594	0.02792	0.01138	0.02002	0.00855	0.01509
GH	0.02209	0.03836	0.01470	0.02550	0.01052	0.01833	0.00793	0.01385
GBM	0.00280	0.00613	0.00276	0.00560	0.00240	0.00474	0.00203	0.00397
HBM	0.00721	0.01391	0.00521	0.01002	0.00394	0.00757	0.00309	0.00593
HTM	0.00415	0.00889	0.00348	0.00711	0.00284	0.00568	0.00232	0.00461
BMG	0.01665	0.02923	0.01119	0.01978	0.00807	0.01433	0.00611	0.01090
BMH	0.02781	0.04779	0.01839	0.03178	0.01309	0.02272	0.00981	0.01708
TMG	0.01846	0.03258	0.01236	0.02194	0.00888	0.01584	0.00671	0.01200
TMH	0.02962	0.05114	0.01956	0.03394	0.01390	0.02422	0.01041	0.01819

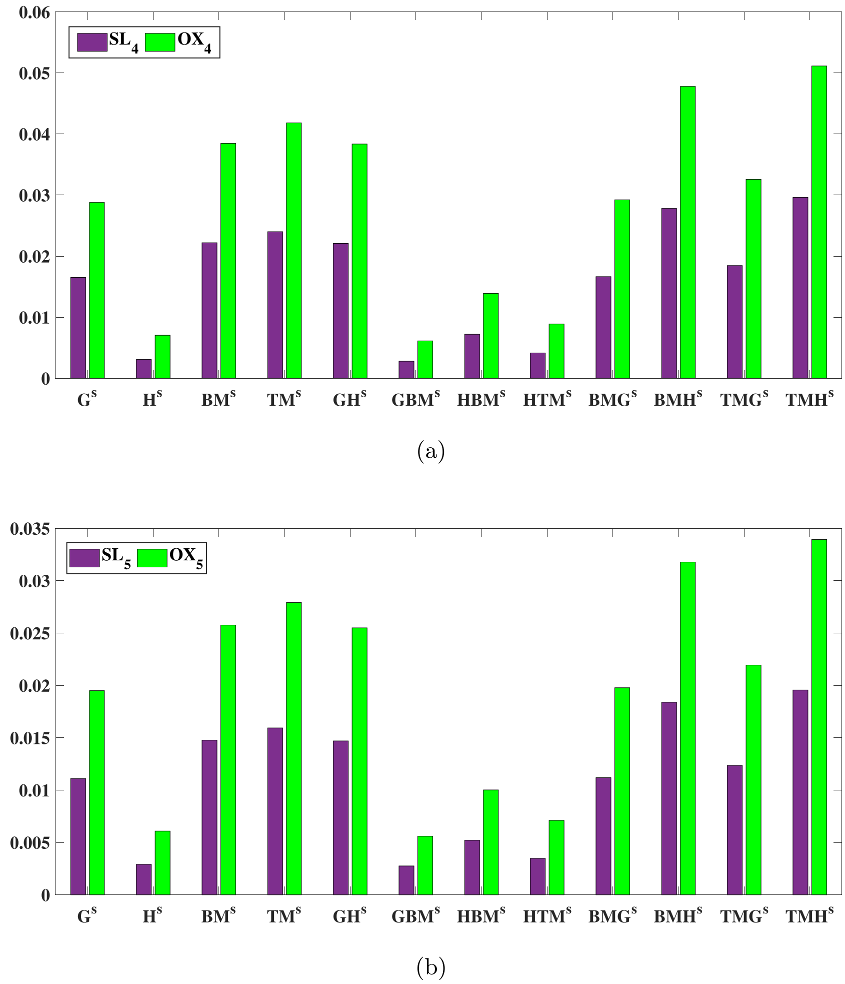

Fig. 6 Comparative graphs of scaled degree-sum entropies between SL_n and OX_n

of bonds in both silicate and oxide frameworks. That is, for the index function χ and $G \in \{SL_n, OX_n\}$,

$$\text{Scaled Entropy of } G = \frac{I_\chi(G)}{|E(G)|}$$

Table 5 provides a detailed comparison between silicate and oxide frameworks, highlighting their bond-wise degree entropies values and emphasizing the consistent higher values of bond-wise entropies in OX_n compared to SL_n as shown in Fig. 5. The trend persists for bond-wise degree-sum entropies, where the scaled entropies are provided in Table 6 and illustrated in Fig. 6.

This comparative analysis serves as a crucial tool in unveiling the relative disorder or randomness within these systems. It provides a quantitative measure, enabling the assessment and ranking of their respective complexities, thereby aiding predictions of stability under varied conditions. Ultimately, this comparative entropy analysis enhances the understanding of silicate and oxide frameworks and their implications in structural properties, facilitating applications in material design and property optimization across various scientific and industrial fields.

4 Conclusion

In this paper, we have investigated topological indices and entropy measures to comprehend the structural characteristics of silicate and oxide frameworks. We have derived the topological expressions for recently proposed indices and conducted a scaled entropy analysis between these two frameworks. Our formulation of topological expressions coupled with scaled entropy has revealed a higher entropy in oxide frameworks relative to their silicate counterparts. This observation highlights the intricate structural arrangements and versatile properties of silicate and oxide frameworks, providing valuable insights for future advancements.

Author Contributions Micheal Arockiaraj and J. Celin Fiona: Conceptualization, methodology, and writing - original draft, J. Celin Fiona and Arul Jeya Shalini: Formal analysis and validation, Micheal Arockiaraj and Arul Jeya Shalini: Visualization. All authors reviewed the manuscript.

Availability of data and materials No data are used for the research.

Declarations

Ethics Approval Not Applicable

Consent to participate Not Applicable

Consent for publication All authors have approved the manuscript and given consent for publication.

Competing interests The authors declare no competing interests.

References

1. Monger HC, Kelly EF (2002) Silica Minerals. Soil mineralogy with environmental applications, soil science society of america. Madison, WI, USA, pp 611–636
2. Götze J (2018) Editorial for special issue mineralogy of quartz and silica minerals. Minerals 8:467
3. Easton A (1972) Chemical analysis of silicate rocks. Elsevier, London, England
4. Samantray J, Anand A, Dash B, Ghosh MK, Behera AK (2022) Silicate minerals - Potential source of potash - A review. Miner Eng 179:107463
5. Hawthorne FC, Uvarova YA, Sokolova E (2019) A structure hierarchy for silicate minerals: sheet silicates. Mineral Mag 83:3–55
6. García-Ruiz JM, Van Zuilen MA, Bach W (2020) Mineral self-organization on a lifeless planet. Phys Life Rev 34–35:62–82
7. Brindavathy R (2022) Silicate minerals induced by microorganisms. Microbiology Monographs. Springer International Publishing, Cham, pp 125–159
8. Jiang N, Shang R, Heijman SGJ, Rietveld LC (2018) High-silica zeolites for adsorption of organic micro-pollutants in water treatment: A review. Water Res 144:145–161
9. Gautam S, Agrawal H, Thakur M, Akbari A, Sharda H, Kaur R, Amini M (2020) Metal oxides and metal organic frameworks for the photocatalytic degradation: A review. J Environ Chem Eng 8:103726
10. Védrine JC (2019) Metal oxides in heterogeneous oxidation catalysis: State of the art and challenges for a more sustainable world. ChemSusChem 12:577–588
11. Zu D-D, Lu L, Liu X-Q, Zhang D-Y, Sun L-B (2014) Improving hydrothermal stability and catalytic activity of metal-organic frameworks by graphite oxide incorporation. J Phys Chem C Nanomater Interfaces 118:19910–19917
12. Védrine JC (2019) Importance, features and uses of metal oxide catalysts in heterogeneous catalysis. Chin J Catalysis 40:1627–1636
13. Gopinath KP, Madhav NV, Krishnan A, Malolan R, Rangarajan G (2020) Present applications of titanium dioxide for the photocatalytic removal of pollutants from water: A review. J Environ Manage 270:110906
14. Manuel P, Rajasingh I (2009) Topological properties of silicate networks. In: GCC Conference & Exhibition 5^{th} IEEE, pp 1–5
15. Manuel P, Rajasingh I (2011) Minimum metric dimension of silicate networks. Ars Comb 98:501–510
16. Arockiaraj M, Kavitha SRJ, Balasubramanian K (2016) Vertex cut method for degree and distance-based topological indices and its applications to silicate networks. J Math Chem 54:1728–1747
17. Arockiaraj M, Kavitha SRJ, Balasubramanian K, Gutman I (2018) Hyper-Wiener and Wiener polarity indices of silicate and oxide frameworks. J Math Chem 56:1493–1510
18. Rajan B, William A, Grigorious C, Stephen S (2012) On certain topological indices of silicate, honeycomb and hexagonal networks. J Comp & Math Sci 3:530–535
19. Hayat S, Imran M (2014) Computation of topological indices of certain networks. Appl Math Comput 240:213–228
20. Liu J-B, Wang S, Wang C, Hayat S (2017) Further results on computation of topological indices of certain networks. IET Control Theory Appl 11:2065–2071
21. Zhang Y-F, Ghani MU, Sultan F, Inc M, Cancan M (2022) Connecting SiO4 in silicate and silicate chain networks to compute kulli temperature indices. Molecules 27:7533
22. Mondal S, De N, Pal A (2019) On some new neighborhood degree-based indices for some oxide and silicate networks. J 2:384–409
23. Baig AQ, Imran M, Ali H (2015) On topological indices of poly oxide, poly silicate, DOX, and DSL networks. Can J Chem 93:730–739
24. Javaid M, Rehman MU, Cao J (2017) Topological indices of rhombus type silicate and oxide networks. Can J Chem 95:134–143
25. Irfan M, Rehman HU, Almusawa H, Rasheed S, Baloch IA (2021) M-polynomials and topological indices for line graphs of chain silicate network and H-naphtalenic nanotubes. J Math 2021:5551825
26. Ediz S (2018) On ve-degree molecular topological properties of silicate and oxygen networks. Int J Comput Sci Math 9:1
27. Akhter S, Imran M, Farahani MR (2019) On topological properties of hexagonal and silicate networks. Hacet J Math Stat 48:711–723
28. Selvarani P, Dhanalakshm K, Catherine JIM (2021) Generalization of new degree based topological indices of Silicate network graph. J Phys Conf Ser 1724:012034
29. Ghani MU, Campena FJH, Ali S, Dehraj S, Cancan M, Alharbi FM, Galal AM (2023) Characterizations of chemical networks entropies by K-banhatii topological indices. Symmetry 15:143
30. Das P, Mondal S, Pal A (2023) Extremal molecular descriptors for oxide and silicate networks. Silicon 15:7565–7577
31. Khan AR, Ghani MU, Ghaffar A, Asif HM, Inc M (2023) Characterization of temperature indices of silicates. Silicon 15:6533–6539
32. Therese SS, Cynthia VJA (2021) Packing of silicate and oxide networks. Mater Today 45:6864–6869
33. Zhang X, Raza A, Fahad A, Jamil MK, Chaudhry MA, Iqbal Z (2020) On face index of silicon carbides. Discrete Dyn Nat Soc 2020:6048438
34. Shirakol S, Kalyanshetti M, Hosamani SM (2019) QSPR analysis of certain distance based topological indices. Appl Math Nonlin Sci 4:371–386
35. Mondal S, De N, Pal A (2022) Topological indices of some chemical structures applied for the treatment of COVID-19 patients. Polycycl Aromat Compd 42:1220–1234
36. Huilgol MI, Sriram V, Udupa HJ, Balasubramanian K (2023) Computational studies of toxicity and properties of β-diketones through topological indices and M/NM-polynomials. Comput Theor Chem 1224:114108
37. Bhatia KS, Gupta AK, Saxena AK (2023) Physicochemical significance of Topological indices: Importance in drug discovery research. Curr Top Med Chem. https://doi.org/10.2174/1568026623666230731103309
38. Arockiaraj M, Paul D, Clement J, Tigga S, Jacob K, Balasubramanian K (2023) Novel molecular hybrid geometric-harmonic-Zagreb degree based descriptors and their efficacy in QSPR studies of polycyclic aromatic hydrocarbons. SAR QSAR Environ Res 34:569–589
39. Arockiaraj M, Greeni AB, Kalaam ARA (2023) Linear versus cubic regression models for analyzing generalized reverse degree based topological indices of certain latest corona treatment drug molecules. Int J Quantum Chem 123:e27136

40. Zhang X, Saif MJ, Idrees N, Kanwal S, Parveen S, Saeed F (2023) QSPR analysis of drugs for treatment of schizophrenia using topological indices. ACS Omega 8:41417–41426
41. Priya S, Tripathi G, Singh DB, Jain P, Kumar A (2022) Machine learning approaches and their applications in drug discovery and design. Chem Biol Drug Des 100:136–153
42. Balasubramanian K (2022) Computational and artificial intelligence techniques for drug discovery and administration. Compr Adv Pharmacol 2:553–616
43. Balasubramanian K (2019) Mathematical and computational techniques for drug discovery: promises and developments. Curr Top Med Chem 18:2774–2799
44. Zhang X, Bajwa ZS, Zaman S, Munawar S, Li D (2023) The study of curve fitting models to analyze some degree-based topological indices of certain anti-cancer treatment. Chem Pap. https://doi.org/10.1007/s11696-023-03143-1
45. Zhang X, Reddy HGG, Usha A, Shanmukha MC, Farahani MR, Alaeiyan M (2023) A study on anti-malaria drugs using degree-based topological indices through QSPR analysis. Math Biosci Eng 20:3594–3609
46. Sabirov DS, Shepelevich IS (2021) Information entropy in chemistry: An overview. Entropy 23:1240
47. Stahura FL, Godden JW, Bajorath J (2002) Differential Shannon entropy analysis identifes molecular property descriptors that predict aqueous solubility of synthetic compounds with high accuracy in binary QSAR calculations. J Chem Inf Comput Sci 42:550–558
48. Yang J, Konsalraj J, Raja SAA (2022) Neighbourhood sum degree-based indices and entropy measures for certain family of graphene molecules. Molecules 28(1):168
49. Govardhan S, Roy S, Balasubramanian K, Prabhu S (2023) Topological indices and entropies of triangular and rhomboidal tessellations of kekulenes with applications to NMR and ESR spectroscopies. J Math Chem 61:1477–1490
50. Shanmukha MC, Usha A, Basavarajappa NS, Shilpa KC (2021) Graph entropies of porous graphene using topological indices. Comput Theor Chem 1197:113142
51. Arockiaraj M, Jency J, Maaran A, Abraham J, Balasubramanian K (2024) Refined degree bond partitions, topological indices, graph entropies and machine-generated boron NMR spectral patterns of borophene nanoribbons. J Mol Struct 1295:136524
52. Jacob K, Clement J, Arockiaraj M, Paul D, Balasubramanian K (2023) Topological characterization and entropy measures of tetragonal zeolite merlinoites. J Mol Struct 1277:134786
53. Rahul MP, Clement J, Junias JS, Arockiaraj M, Balasubramanian K (2022) Degree-based entropies of graphene, graphyne and graphdiyne using Shannon's approach. J Mol Struct 1260:132797
54. Zhang X, Siddiqui MK, Javed S, Sherin L, Kausar F, Muhammad MH (2022) Physical analysis of heat for formation and entropy of ceria oxide using topological indices. Comb Chem High Throughput Screen 25:441–450
55. Govardhan S, Roy S (2023) Topological analysis of hexagonal and rectangular porous graphene with applications to predicting π-electron energy. Eur Phys J Plus 138:670
56. Yang J, Fahad A, Mukhtar M, Anees M, Shahzad A, Iqbal Z (2023) Complexity analysis of Benes network and its derived classes via information functional based entropies. Symmetry 15:761
57. Zhang X, Rauf A, Ishtiaq M, Siddiqui MK, Muhammad MH (2022) On degree based topological properties of two carbon nanotubes. Polycycl Aromat Compd 42:866–884
58. Zhong J-F, Rauf A, Naeem M, Rahman J, Aslam A (2021) Quantitative structure-property relationships (QSPR) of valency based topological indices with Covid-19 drugs and application. Arab J Chem 14:103240
59. Kavitha SRJ, Abraham J, Arockiaraj M, Jency J, Balasubramanian K (2021) Topological characterization and graph entropies of tessellations of kekulene structures: Existence of isentropic structures and applications to thermochemistry, NMR and ESR. J Phys Chem A 125:8140–8158
60. Abraham J, Arockiaraj M, Jency J, Kavitha SRJ, Balasubramanian K (2022) Graph entropies, enumeration of circuits, walks and topological properties of three classes of isoreticular metal organic frameworks. J Math Chem 60:695–732
61. Mushtaq S, Arockiaraj M, Fiona JC, Jency J, Balasubramanian K (2022) Topological properties, entropies, stabilities and spectra of armchair versus zigzag coronene-like nanoribbons. Mol Phys 120:e2108518

Publisher's Note Springer Nature remains neutral with regard to jurisdictional claims in published maps and institutional affiliations.

Springer Nature or its licensor (e.g. a society or other partner) holds exclusive rights to this article under a publishing agreement with the author(s) or other rightsholder(s); author self-archiving of the accepted manuscript version of this article is solely governed by the terms of such publishing agreement and applicable law.